25th ABCM International Congress of Mechanical Engineering
October 20-25, 2019, Uberlândia, MG, Brazil

COB-2019-0855
MATHEMATICAL AND COMPUTATIONAL MODELING OF THE TWO-DIMENSIONAL FLOW THROUGH A POROUS SQUARE CYLINDER DOWNSTREAM A BACKWARD-FACING STEP

Ítalo Augusto Magalhães de Ávila
Gabriel Machado dos Santos
Hélio Ribeiro Neto
Aristeu da Silveira Neto
Federal University of Uberlândia, Av. João Naves de Ávila 2121, Campus Santa Mônica. Uberlândia, MG, Brazil, CEP 38400-902.
italo.ufuracing@gmail.com, gabriel.msantos@ufu.br, heliorine@hotmail.com, aristeus@ufu.br

Abstract. *In this paper the authors present the physical, mathematical and computational modeling of the laminar flow through a square cylinder composed of a porous medium downstream a backward-facing step. The modeling equations are solved in a two-dimensional fixed Eulerian and Cartesian domain through the finite-difference method. Streamlines and velocity profiles are presented for different values of porosity and permeability.*

Keywords: *computational fluid dynamics, numerical simulation, porous media, backward-facing step*

1. INTRODUCTION

The backward-facing step case (BFS) is extensively studied in the literature for the evaluation of separating, recirculating and reattaching flow, characteristics present in numerous engineering applications. Some studies demonstrate the enhancement of thermal energy transfer due to the mixing of high and low energy particles in reattachment regions. The presence of an obstacle downstream a step affects significantly mass and thermal energy transport due to uneven pressure and temperature distributions, and this case in particular has received less attention. In this context, the present work aims the evaluation of the effects of a porous square cylinder downstream a backward-facing step over the flow, that up to this date, to the best knowledge of the authors, has not been explored.

The mechanics of flows through porous media are traditionally emulated according to the empirical Darcy-Forchheimer model, which describes the macroscopic effects of the fluid's interaction with the porous structure through the conciliation of inertial and viscous effects (linear and non-linear corrections). In its mathematical form, the contact force is modeled as a function of porosity, permeability and experimental constants, related to the medium's geometric characterization. This methodology can be found in the works of Guo and Zhao (2002), Vafai (2005), Dhinakaran and Ponmozhi (2011), Liu and He (2017), Mahdhaoui *et al.* (2017) and Luo and Xu (2019).

Although the geometry of the porous structure presented in this paper is canonical, its interaction with the fluid can offer significant insights of features such as flow separation, wake formation and thermal distribution. Information of great interest for the design of cooling towers and dump combustors, for instance. Some effort was invested in similar analysis for solid geometries, as observed in the works of Selimefendigil and Oztop (2014) and Chattergee *et al.* (2015).

An in-house code was developed and simulations were conducted in order to evaluate the individual influence of parameters such as porosity and permeability (Darcy's number) over the flow. The modeling equations are solved in a two-dimensional fixed Eulerian and Cartesian domain through the finite-difference method.

2. PHYSICAL AND DIFFERENTIAL MODELING

For the modeling of the flow through a porous square cylinder downstream a backward-facing step, it is possible to model the fluid as Newtonian and the flow as incompressible. The solid phase physical properties are modeled as homogeneous and isotropic through the domain. A graphic representation of the domain and of the boundary conditions is presented at Fig.(1), in which D represents the edge of the porous square and L represents a given dimension of the domain in function of the step size ($h = L_{left}$), so that $L_{bl} = 20\ h$, $L_{br} = 52\ h$ and $L_{right} = 2\ h$. The obstacle is fixed at $x_c = 2D$ and $y_c = h$.

For the differential modeling of fluid mechanics, the application of Reynolds transport theorem, Newton's second law and energy balance in a differential volume, provide the relations required to describe the movement of the fluid and evaluate the energy transport and transformations. The first, when employed to the analysis of the mass flux through a

control volume (REV), provides the continuity equation, which ensures that the mass balance will be respected. The linear momentum equations (or Navier-Stokes equations) are obtained from Newton's second law, that presents the relation between the acceleration perceived by the system and the external forces acting upon it. Finally, the solution of the temperature field is possible through the thermal energy balance in a control volume (differential energy equation).

The differential and numerical modeling of the thermal energy transport is presented. This paper, however, is dedicated to the linear momentum transport analysis. In this sense, it is convenient to consider a null gravitational field, so that the solution of the thermal field is not associated, through gravitational effects, to the linear momentum transport phenomena.

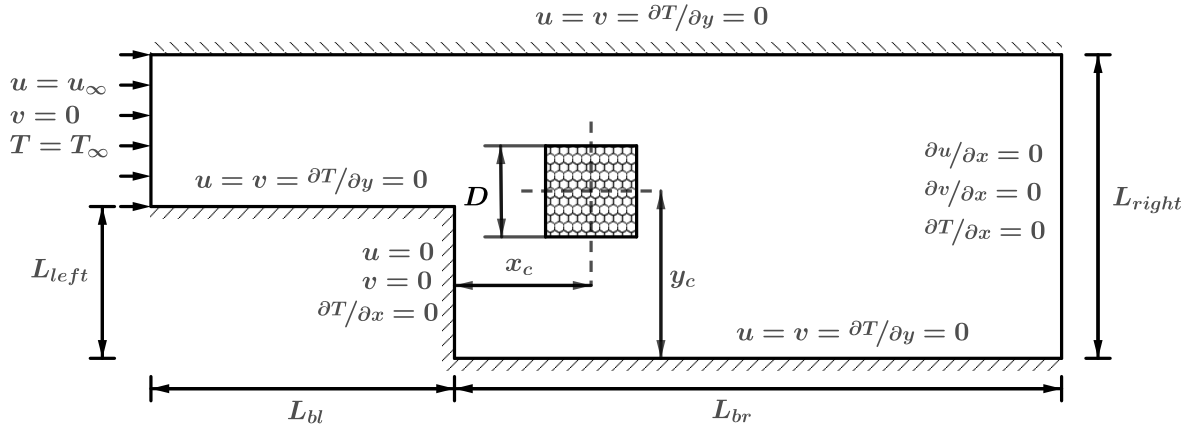

Figure 1: Graphic representation of the boundary conditions.

For the modeling of flows through isotropic porous media, the Darcy-Forchheimer empirical model proposes the addition of a source therm for the linear momentum equation, described as follows.

$$-\boldsymbol{\nabla} P_{pore} = \frac{\mu \mathbf{V}}{K} + \frac{F\rho|\mathbf{V}|\mathbf{V}}{\sqrt{K}}, \tag{1}$$

where $\boldsymbol{\nabla} P_{pore}$ is the pressure drop due to the interaction with the porous medium, μ the fluid dynamic viscosity, K the permeability, $\mathbf{V}$ the velocity vector, ρ the specific mass of the fluid and F the Forchheimer coefficient (function of porosity and microscopic solid geometry).

For the modeling of the thermal phenomena, the differential thermal energy equation must account for the conduction, by both fluid and solid phases, and the advection, which occurs only for the fluid phase. Physical properties of the porous medium may be estimated by their volumetric average, function of the porosity (ratio between fluid and total volume in the system).

$$(\rho C)_m = \varepsilon (\rho C)_f + (1-\varepsilon)(\rho C)_s, \tag{2}$$

$$k_m = \varepsilon k_f + (1-\varepsilon) k_s, \tag{3}$$

where the subscripts f, s and m refer to the properties of fluid, solid and porous medium, respectively. The specific thermal capacity is given by C, the thermal conductivity coefficient by k, and the porosity by ε.

The continuity, linear momentum and energy equations for the flow through an isotropic porous media are presented bellow:

$$\boldsymbol{\nabla} \cdot \mathbf{V} = 0, \tag{4}$$

$$\frac{1}{\varepsilon}\frac{\partial \mathbf{V}}{\partial t} + \frac{1}{\varepsilon^2}(\mathbf{V}\cdot\boldsymbol{\nabla})\mathbf{V} = -\frac{1}{\rho}\boldsymbol{\nabla} p - \mathbf{g}\beta(T - T_o) + \frac{\nu}{\varepsilon}\boldsymbol{\nabla}^2\mathbf{V} - \frac{\nu}{K}\mathbf{V} - \frac{F|\mathbf{V}|\mathbf{V}}{\sqrt{K}}, \tag{5}$$

$$(\rho C)_m \frac{\partial T}{\partial t} + (\rho C)_f \mathbf{V}\cdot\boldsymbol{\nabla} T = k_m \boldsymbol{\nabla}^2 T, \tag{6}$$

where p represents the pressure, $\mathbf{g}$ the gravitational field, β the thermal expansion coefficient, ν the kinematic viscosity (ratio of the viscosity to the specific mass), T the volume averaged temperature (fluid and solid phases jointly) and T_o the reference temperature. With this set of equations the incompressible flows of newtonian fluids through an homogeneous porous medium in transient regime are modeled.

For the modeling of the flow through non-porous regions, the Darcy-Forchheimer correction and the thermal tortuosity effects are suppressed, and the Eq.(5) and (6) are reduced to the classical Navier-Stokes equations and the differential thermal energy equation, presented bellow:

$$\frac{\partial \mathbf{V}}{\partial t} + (\mathbf{V}\cdot\boldsymbol{\nabla})\mathbf{V} = -\frac{1}{\rho}\boldsymbol{\nabla} p - \mathbf{g}\beta(T - T_o) + \nu\boldsymbol{\nabla}^2\mathbf{V}, \tag{7}$$

$$(\rho C)_f \frac{\partial T}{\partial t} + (\rho C)_f \mathbf{V} \cdot \boldsymbol{\nabla} T = k_f \boldsymbol{\nabla}^2 T. \tag{8}$$

The non-isothermal constant inlet velocity flow over an immersed body is usually characterized by the Reynolds number ($Re = \rho V D/\mu$) and the Prandtl number ($Pr = \nu/\alpha$). Considering that the body consists of a porous medium, parameters such as the conductivity ratio ($\lambda = k_f/k_m$), Darcy number ($Da = K/L^2$) and porosity (ε) must also be accounted for. The symbol α represents the thermal diffusivity.

3. NUMERICAL MODEL

With the physical and differential models defined, a numerical model can be used to obtain an approximate solution to this problem. The domain is discretized evenly and Taylor's expansion is used to the approximation of both first (CDS) and second order derivatives. For a function in a two-dimensional space the domain may be written as follows:

$$\mathcal{M} = \{(t^N, x_I, y_J);\ t^N = N\Delta t,\ x_I = I\Delta x,\ y_J = J\Delta y,\ N = 0, 1, \ldots, K,\ I = 0, 1, \ldots, L,\ J = 0, 1, \ldots, M\} \tag{9}$$

The equations presented previously can only be applied to a continuous domain and must be rewritten. The modified value for the horizontal and vertical velocity components ($\hat{u}$ and $\hat{v}$, respectively) are obtained from the following equations:

$$\begin{aligned}\hat{u}_{I,J} = &-(\varepsilon\,\delta_p + \delta_f)\,\Delta t\beta\left[\frac{T^N_{I-1,J} + T^N_{I,J}}{2T_o} - 1\right] g_x - (\varepsilon\,\delta_p + \delta_f)\,\frac{\Delta t}{\rho}\,\frac{p^N_{I,J} - p^N_{I-1,J}}{\Delta x} - \\ &\frac{\Delta t}{\varepsilon\,\delta_p + \delta_f}\,u^N_{I,J}\,\frac{u^N_{I+1,J} - u^N_{I-1,J}}{2\Delta x} - \frac{\Delta t}{\varepsilon\,\delta_p + \delta_f}\,v^N_{I,J}\,\frac{u^N_{I,J+1} - u^N_{I,J-1}}{2\Delta x} - \varepsilon\,\delta_p \frac{F|V^N_{I,J}|u^N_{I,J}}{\sqrt{K}} + \\ &\frac{\Delta t\,\mu}{\rho}\,\frac{u^N_{I+1,J} - 2u^N_{I,J} + u^N_{I-1,J}}{\Delta x^2} + \frac{\Delta t\,\mu}{\rho}\,\frac{u^N_{I,J+1} - 2u^N_{I,J} + u^N_{I,J-1}}{\Delta y^2} - \varepsilon\,\delta_p \frac{\mu}{\rho K} u^N_{I,J} + u^N_{I,J},\end{aligned} \tag{10}$$

$$\begin{aligned}\hat{v}_{I,J} = &-(\varepsilon\,\delta_p + \delta_f)\,\Delta t\beta\left[\frac{T^N_{I,J-1} + T^N_{I,J}}{2T_o} - 1\right] g_y - (\varepsilon\,\delta_p + \delta_f)\,\frac{\Delta t}{\rho}\,\frac{p^N_{I,J} - p^N_{I,J-1}}{\Delta y} - \\ &\frac{\Delta t}{\varepsilon\,\delta_p + \delta_f}\,v^N_{I,J}\,\frac{v^N_{I,J+1} - v^N_{I,J-1}}{2\Delta y} - \frac{\Delta t}{\varepsilon\,\delta_p + \delta_f}\,u^N_{I,J}\,\frac{v^N_{I+1,J} - v^N_{I-1,J}}{2\Delta x} - \varepsilon\,\delta_p \frac{F|V^N_{I,J}|v^N_{I,J}}{\sqrt{K}} + \\ &\frac{\Delta t\,\mu}{\rho}\,\frac{v^N_{I+1,J} - 2v^N_{I,J} + v^N_{I-1,J}}{\Delta x^2} + \frac{\Delta t\,\mu}{\rho}\,\frac{v^N_{I,J+1} - 2v^N_{I,J} + v^N_{I,J-1}}{\Delta y^2} - \varepsilon\,\delta_p \frac{\mu}{\rho K} v^N_{I,J} + v^N_{I,J},\end{aligned} \tag{11}$$

where δ_p and δ_f are Kronecker delta functions used to mark porous and non-porous regions, respectively.

The correction for the pressure (p^o) is obtained from the continuity equation, as indicated in Eq. (12), and the value of the velocity components must be corrected from its modified value through this correction. The pressure field is logged at each time step as presented in Eq. (14).

$$\boldsymbol{\nabla}^2 p^o = \boldsymbol{\nabla} \cdot \mathbf{V} \approx \frac{\hat{u}_{I+1,J} - \hat{u}_{I,J}}{\Delta x} + \frac{\hat{v}_{I,J+1} - \hat{v}_{I,J}}{\Delta y}, \tag{12}$$

$$u^{N+1}_{I,J} = \hat{u}_{I,J} - \frac{p^o_{I,J} - p^o_{I-1,J}}{\Delta x}, \tag{13}$$

$$p_{I,J} = p_{I,J} + p^o_{I,J}. \tag{14}$$

The energy equation, in its turn, can be rewritten as indicated bellow. In Eq. (15), the parameters $\check{u}$ and $\check{v}$ represent the interpolated velocity components.

$$\begin{aligned}T^{N+1}_{I,J} = &\Delta t(\delta_f \alpha_f + \delta_p \alpha_m)\left[\frac{T^N_{I+1,J} - 2T^N_{I,J} + T^N_{I-1,J}}{\Delta x^2} + \frac{T^N_{I,J+1} - 2T^N_{I,J} + T^N_{I,J-1}}{\Delta y^2}\right] - \\ &\frac{\Delta t(\rho C)_f}{\delta_f(\rho C)_f + \delta_p(\rho C)_m}\left[\check{u}^N_{I,J}\,\frac{T^N_{I+1,J} - T^N_{I-1,J}}{2\Delta x} - \check{v}^N_{I,J}\,\frac{T^N_{I,J+1} - T^N_{I,J-1}}{2\Delta x}\right] + T^N_{I,J}.\end{aligned} \tag{15}$$

4. RESULTS AND DISCUSSIONS

In this section, the results obtained with the developed computational model for the two-dimensional, laminar and incompressible flow through a porous square cylinder are presented. Simulations are conducted for fixed values of the Reynolds and Prandtl numbers ($Re = 100$, $Pr = 0.71$) and the boundary conditions previously defined.

Higher values of Darcy's number, in a medium of constant porosity, are associated to solid particles of more significant characteristic lenghts. The mathematical relation between the parameters is presented by Ergun (1952). This property can be explained by the fact that, for a given volume, both projected and superficial areas are increased with the number of particles that compose it. Such a condition implies an inverse proportionality between the contact force, due to inertial and viscous effects, function of projected and superfial areas, and Darcy's number.

In a medium of constant permeability, however, different values of porosity are associated simultaneously with different characteristic lengths and volumetric proportions between phases. For a given value of Darcy, an increase in porosity, or a decrease in the solid phase volumetric proportion within the porous matrix, must be related to an increase in the number of particles. Reductions in the value of the porosity are intuitively associated with reductions in the resistance that the medium exerts to the movement of the fluid by its borders and in its interior. However, the increase in the number of particles is associated with an increase in forces due to inertial and viscous effects.

It is expected, according to these considerations, that, of the two parameters, Darcy's number is more influential over the flow's characteristics. In order to evaluate the validity of the argumentation, for a Darcy number of 10^{-2}, simulations are conducted for the porosity values of 0.1, 0.2, 0.5 and 0.9. For a fix porosity of 0.1, simulations are conducted for the Darcy values of 10^{-4}, 10^{-3}, 10^{-2} and 10^{-1}. It should be noted that the characteristic dimension for the calculation of the dimensionless Reynolds in this case does not correspond to the edge of the cylinder, but to the L_{right} dimension of the channel.

An uniform spatial increment of approximately $6.67\ mm$ and a fixed time step of $10^{-4}\ s$ are defined for the numerical simulations. Probes are positioned along cross-sections of the channel in order to evaluate the impact of each parameter over the linear momentum transport. The velocity profiles obtained are presented at Figs.(2) and (3). The streamlines, plotted over the velocity magnitude, are presented at Figs.(4) and (5). Reattaching lengths for the different configurations are presented at Fig.(6).

It is observed that, in fact, the reattaching length is affected more significantly by the Darcy number. It is interesting to note that, for the simulated cases, the increase of the porosity provided a reduction in the recirculating length. The inertial and viscous effects, that are amplified with the increase in the number of solid particles (consequent of an increase in the porosity), are more significant over the linear momentum transport than the decrease in the volumetric fraction of the solid phase.

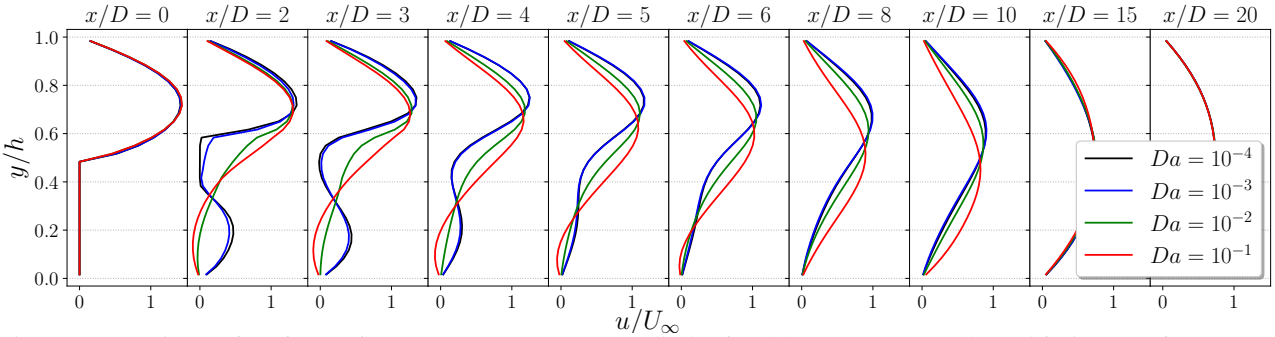

Figure 2: Velocity profiles for the flow over a porous square cylinder fixed downstream a backward facing step for $\varepsilon = 0.1$, $Re = 100$ and different values of the Darcy number.

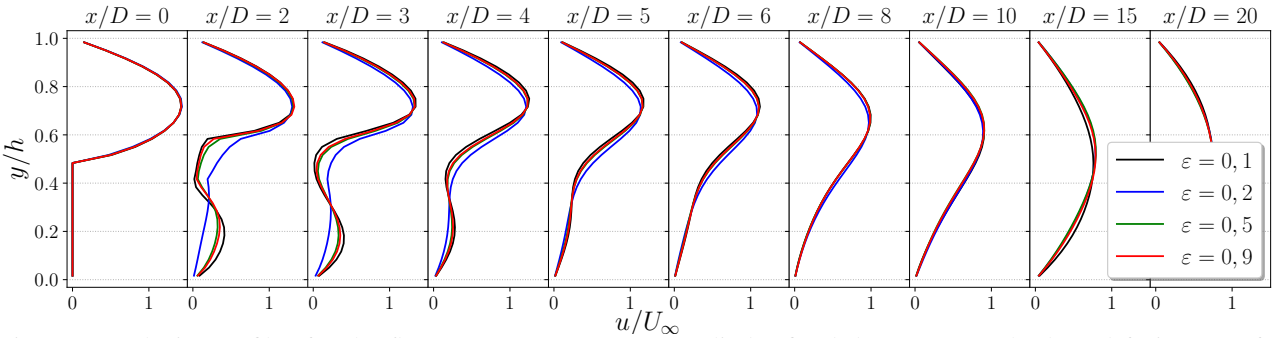

Figure 3: Velocity profiles for the flow over a porous square cylinder fixed downstream a backward facing step for $Da = 10^{-2}$, $Re = 100$ and different values of porosity.

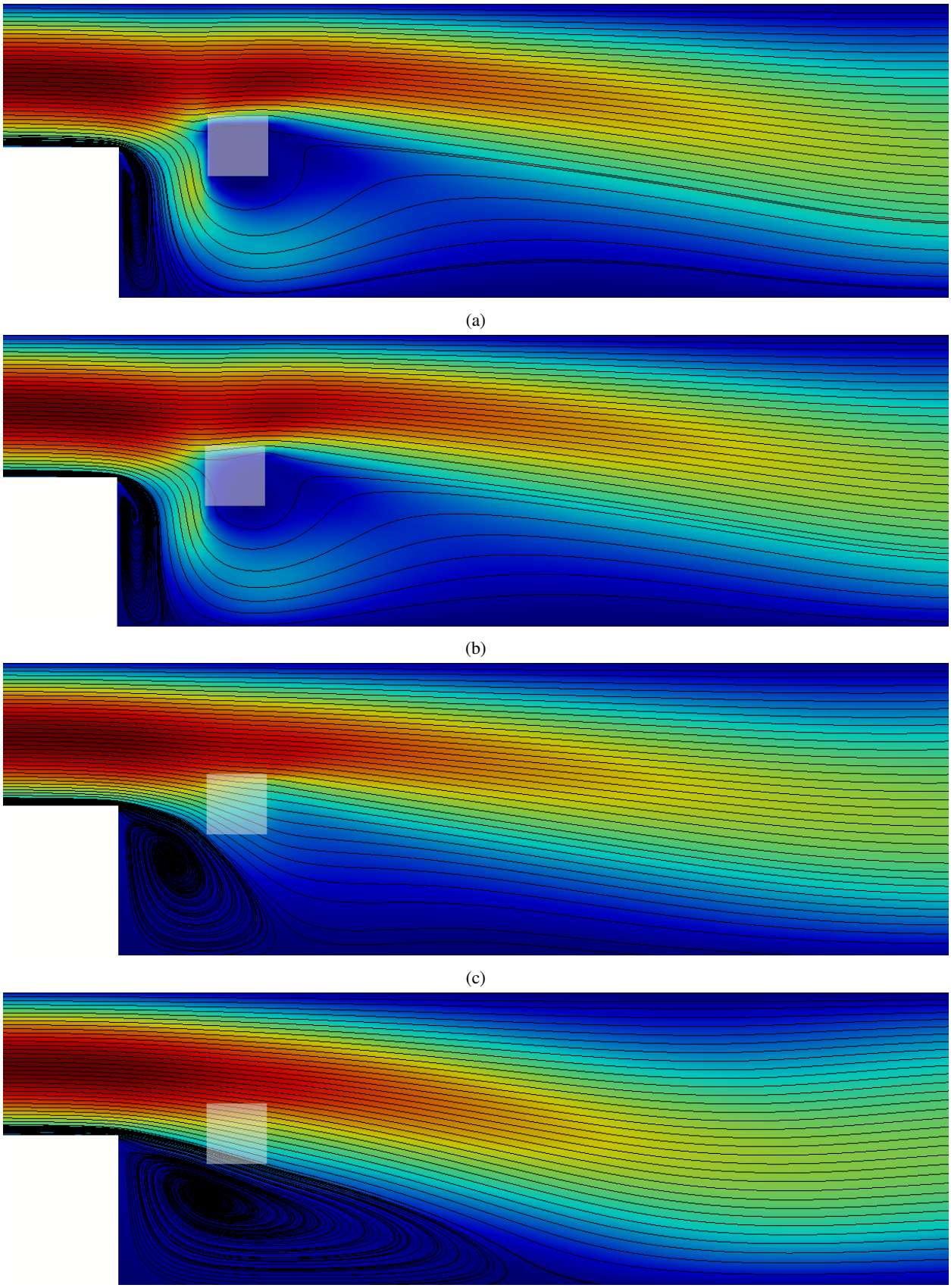

(a)

(b)

(c)

(d)

Figure 4: Streamlines for the flow over a porous square cylinder fixed downstream a backward facing step at $t = 10\ s$ for $Re = 100$, $\varepsilon = 0.1$: (a) $Da = 10^{-4}$, (b) $Da = 10^{-3}$, (c) $Da = 10^{-2}$, (d) $Da = 10^{-1}$.

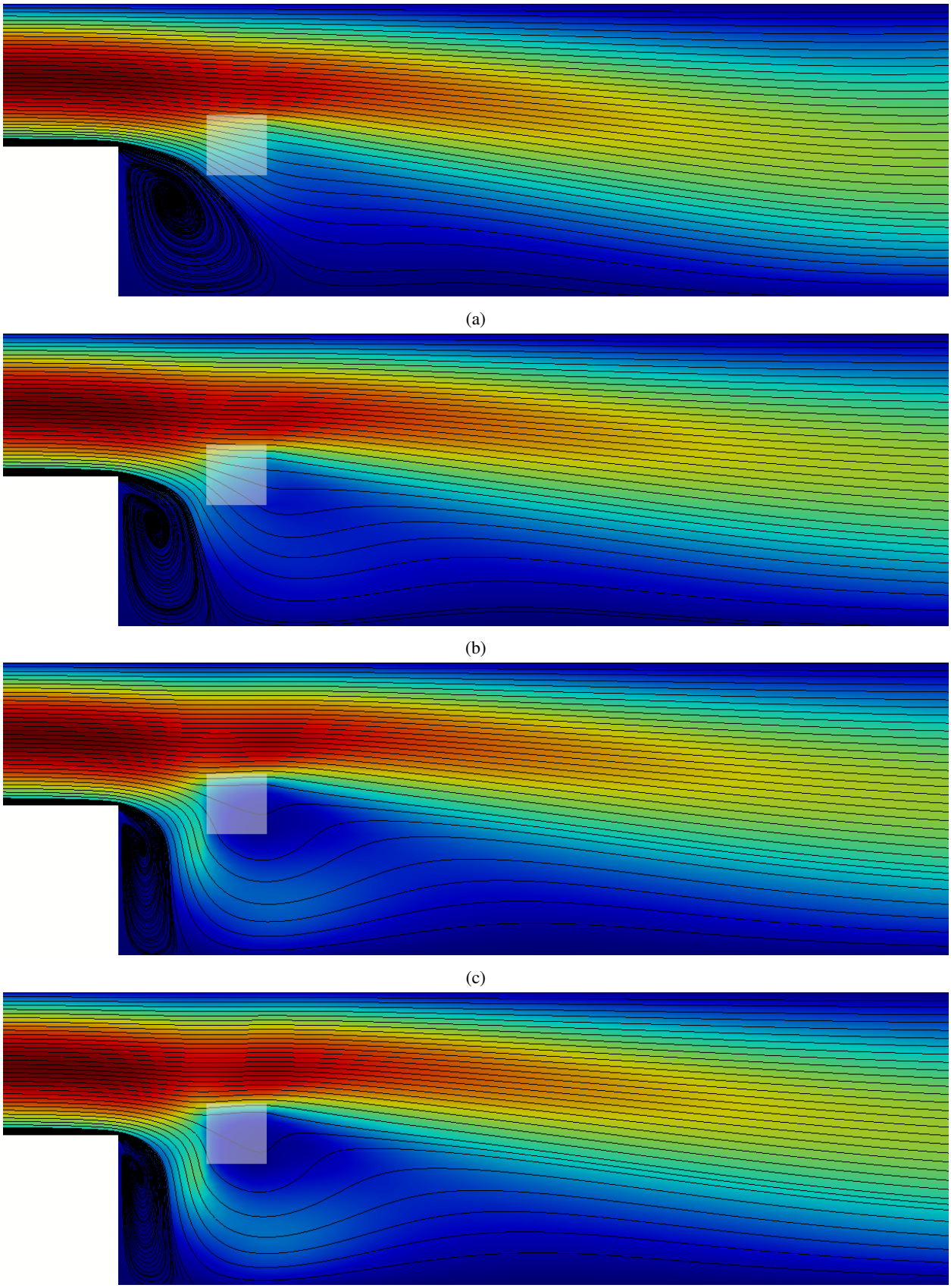

(a)

(b)

(c)

(d)

Figure 5: Streamlines for the flow over a porous square cylinder fixed downstream a backward facing step at $t = 10\ s$ for $Re = 100$, $Da = 10^{-2}$: (a) $\varepsilon = 0.1$, (b) $\varepsilon = 0.2$, (c) $\varepsilon = 0.5$, (d) $\varepsilon = 0.9$.

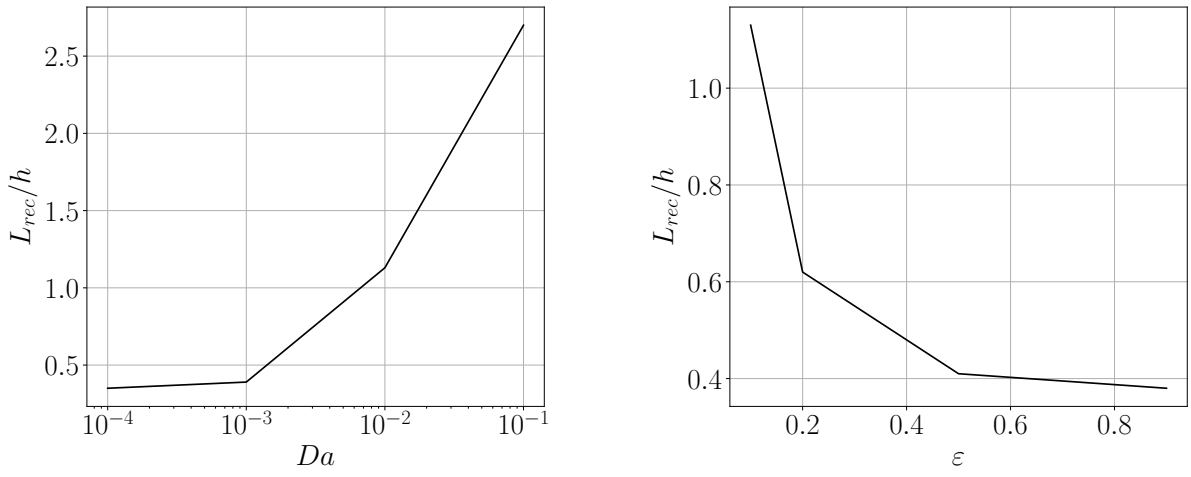

(a) $\varepsilon = 0.1$ (b) $Da = 10^{-2}$

Figure 6: Reattachment lenght for different values of porosity and permeability of a porous square cylinder fixed downstream a backward facing step.

5. CONCLUSION

The modeling of mass, energy and linear momentum transport phenomena in the laminar flow through a porous structure downstream a backward-facing step was presented. A computational model was developed and simulations were conducted aiming the evaluation of the flow's characteristics in function of the medium's porosity and permeability. The results indicate that, of these parameters, the latter is the most influential over the linear momentum transport phenomena.

It is convenient to point that a reduction in the volumetric fraction of the solid phase is not necessarily associated to greater permissivities to the flow through a porous structure. For the configurations modeled in the present work, an increase in the value of the porosity provided an increase in the medium's resistance to the movement of the fluid. Such is an extremely pertinent remark in the design of porous mechanical components, in which both permeability and mechanical resistance are relevant.

6. ACKNOWLEDGEMENTS

The authors would like to thank PROPP-UFU, CNPq, CAPES, FAPEMIG, and Petrobras S.A. for financial and material support.

7. REFERENCES

Chattergee, D., Sengupta, A., Debnath, N. and De, S., 2015. "Influence of an adiabatic square cylinder on hydrodynamic and thermal characteristics in two-dimensional backward-facing step channel". *Heat Transfer Research*, Vol. 46, No. 1, pp. 63–89.

Dhinakaran, S. and Ponmozhi, J., 2011. "Heat transfer from a permeable square cylinder to a flowing fluid". *Energy Conversion and Management*, Vol. 52, No. 1, pp. 2170–2182.

Ergun, S., 1952. "Fluid flow through packed columns". *Chemical Engineering Progress*, Vol. 48, No. 1, pp. 89–94.

Guo, Z. and Zhao, T.S., 2002. "Lattice boltzmann model for incompressible flows through porous media". *Physical Review*, Vol. 66, No. 036304, pp. 1–9.

Liu, Q. and He, Y.L., 2017. "Lattice boltzmann simulations of convection heat transfer in porous media". *Physica A*, Vol. 46, No. 1, pp. 742–753.

Luo, Z. and Xu, H., 2019. "Numerical simulation of heat and mass transfer through microporous media with lattice boltzmann method". *Thermal Science and Engineering Progress*, Vol. 9, No. 1, pp. 44–51.

Mahdhaoui, H., Chesneau, X. and Laatar, A.H., 2017. "Numerical simulation of flow through a porous square cylinder". *Energy Procedia*, Vol. 139, No. 1, pp. 785–790.

Selimefendigil, F. and Oztop, H.F., 2014. "Control of laminar pulsating flow and heat transfer in backward-facing step by using a square obstacle". *Journal of Heat Transfer*, Vol. 136, No. 081701, pp. 1–11.

Vafai, K., 2005. *Handbook of Porous Media*. Taylor & Francis Group, 6000 Broken Sound Parkway NW, Suite 300, 2nd edition.

8. RESPONSIBILITY NOTICE

The authors are the only responsible for the printed material included in this paper.